Pathways to charge equilibration following multiple electron exchange between highly charged ions and atoms

de Nijs, Gerardus

Chapter 5

Pathways to charge equilibration in C^{6+}-Ar collisions studied by electron target-ion coincidences

Abstract *We present electron spectra resulting from collisions of $^{13}C^{6+}$ on Ar. Partial electron spectra are determined in coincidence with the charge state of the resulting Ar-ion. The interpretation of the electron spectra shows evidence for target excitation. The electron spectra in coincidence with Ar^{3+}, Ar^{4+}, Ar^{5+} target ions show that, despite the initially populated manifold, the energies of autoionizing decaying electrons lie in the same range. The corresponding decay pathways are compared with the predictions of the overbarrier model.*

5.1 Introduction

The general features of electron capture by highly charged ions from neutral gas targets can be well described by the classical overbarrier model (Niehaus 1986). The initial population of highly excited states turn out to be well predicted for one- and two-electron capture processes (Chen and Lin 1987, Mack 1989, Bordenave-Montesquieu 1987, Posthumus *et al* 1992). In some collision systems it was found that for two-electron capture an unexpectedly large fraction of doubly excited states decays radiatively (Roncin *et al* 1991). This observation has motivated many theoretical (Van der Hart *et al* 1995, Roncin *et al* 1993,

Van der Hart and Hansen 1994) and experimental (Bachau *et al* 1992, Martin *et al* 1993, Ali *et al* 1993) investigations. Often multi-electron targets were used to study radiative stabilization. A problem with multi-electron targets is that the experiments should distinguish processes according to the number of transferred electrons, i.e. the target charge state. In N^{7+} on Ar collisions, a system with an enhanced radiative stabilization ratio, we showed (De Nijs *et al* 1994, chapter 4), using an electron-target ion coincidence technique, that besides the population of the doubly excited states which give rise to radiative stabilization, also more strongly bound states are populated during double electron capture processes. The capture into strongly bound doubly excited states takes place from inner target orbitals. It was found that capture of electrons more strongly bound than the outermost electrons, is of importance in understanding the electron capture dynamics with highly charged ions. It was shown (De Nijs *et al* 1996, chapter 6) that for different collision systems even *inner-shell* electron capture is important in electron capture processes.

In this chapter we report on the autoionization electron spectra arising from collisions between $^{13}C^{6+}$ and Ar, measured in coincidence with the target charge state. The interpretation of the spectra leads to the conclusion that also in this collision system for two-electron capture processes target excitation is an important effect. For multi-electron capture we find that autoionizing decay yields electrons in the same energy range despite the larger number of initially captured electrons. By means of Hartree-Fock calculations we have determined binding energies of the various multiply excited states involved. Using these calculations in combination with the ion-electron coincidence measurements it is possible to unravel the spectra and to identify the various pathways along which electron capture, electron emission and subsequent stabilization of the collision partners proceeds. It turns out that these pathways are in agreement with the predictions of the classical overbarrier model (Niehaus 1986).

5.2 Experiment

Highly charged $^{13}C^{6+}$ are extracted from an ECR ion source installed at the KVI Atomic Physics facility. To produce pure $^{13}C^{6+}$ isotopic carbonmonoxide is used to avoid He^{2+} beam contributions produced from He, which is used as mixing gas in the ECR ion source. The ion source can operate between 2 and 20 kV. The highly charged ions are transported to a setup containing an electron spectrometer and a target ion charge state analyzer (Posthumus and Morgenstern 1992, chapter 3). In forward direction under an angle of $50.0 \pm 2.4^{\circ}$, we measure the autoionization electrons. By applying a small voltage to the reaction centre the target ions are extracted in backward direction. The time-of-flight from reaction centre to the ion detector allows to determine the charge state of the target ion. More details of the experiments are outlined in chapter 3 The detection of an electron serves as a start and that of an ion as a stop for the time measurement. The measured coincidence spectrum are background subtracted and transformed into the emitter frame.

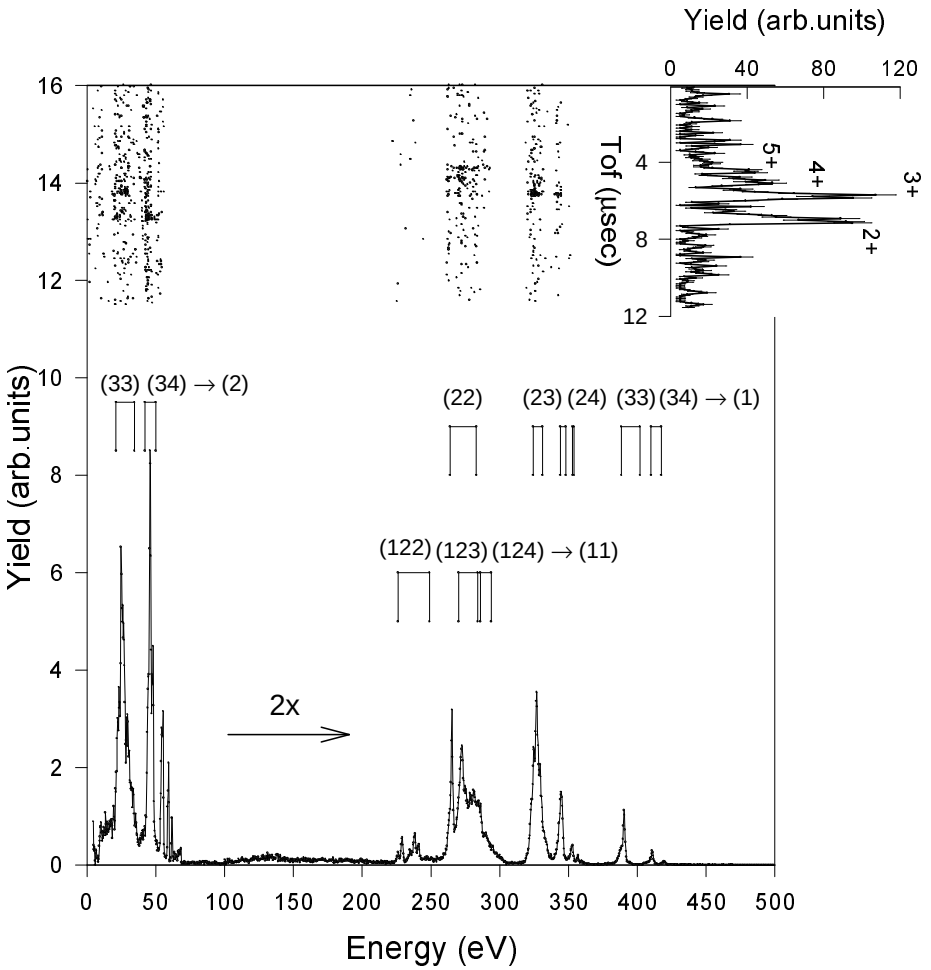

Figure 5.1: In the top part of the figure the coincidence measurements of $^{13}C^{6+}$ on Ar are presented. The horizontal axis of this scattergram represents the electron energy, the vertical one is the time-of-flight of the target ions. Each dot in the scattergram means that at least two events were measured. In the bottom part of the figure the non-coincident electron spectrum is plotted. Also indicated are various peak identifications. The part above 100 eV is magnified by a factor two.

5.3 Experimental results

In figure 5.1 we have plotted the results of the coincidence measurements of $^{13}C^{6+}$ on Ar at a collision energy of 4.67 keV amu^{-1}. The horizontal axis corresponds to the electron energy, while the vertical one gives the time-of-flight of the ions. Each dot in the figure indicates that at least two electron-ion coincidence events have been measured. In the lower part of the figure we have plotted the singles measurements. This spectrum is corrected for Doppler shift and transmission of the spectrometer. Clearly seen are the structures corresponding to different initially populated states. It is remarkable that none of the high energy electrons (>100 eV) is coincident with Ar^{2+} target ions. Moreover the high energy electrons can often not uniquely be ascribed to only one target charge state, but arise from three- as well as four- and five electron capture.

From the coincidence scattergram it is possible, after background subtraction, to extract partial electron spectra, i.e. electron spectra in coincidence with a specific final charge state of the target. For collisions between $^{13}C^{6+}$ and Ar, the partial spectrum in coincidence with Ar^{2+} is plotted in figure 5.2, while the electron spectrum in coincidence with Ar^{3+} is plotted in figure 5.3. For coincidences of electrons with Ar^{4+} and Ar^{5+} the high electron energy parts of the spectra are plotted in figure 5.5 and 5.7.

5.4 Discussion

In the first place we will try to describe the features of the various capture processes in terms of the overbarrier model (Niehaus 1986). Details of the model can be found in chapter 2. For a given collision system the model predicts binding energies of the electrons, principal quantum numbers and reaction windows. These reaction windows are taken to be Gaussian shaped probability distributions centered around the most probable binding energy of the final state. The width of the window depends on the collision velocity and the distances at which capture takes place. Different processes are labeled with so-called strings. For instance the string {11010} indicates that five electrons become quasi-molecular during the collision and that the first (the most loosely bound electron), second and fourth electron are captured by the projectile and that the third and fifth electron (the most strongly bound one of the five electrons) are recaptured by the target. The binding energies of different electronic configurations in the ion are calculated with self-consistent Hartree-Fock calculations, using the Cowan-code (Cowan 1981).

The excited projectile states decay primarily via cascades of autoionization electrons. For example, four electron capture leads to a two-fold ionized projectile C^{2+}. Autoionizing cascades lead to electron emission and will stepwise increase the projectile charge until the ground state is reached. Qualitatively one can expect that capture of different numbers of electrons may result in autoionization electrons at comparable energies, since analogue transitions may take place in the projectile with or without additionally captured 'spectator'

electrons, which have only a marginal influence on the emitted electron energies.

The first cascade in the decay increases the charge and is accompanied by electron emission. The next autoionizing cascade step of C^{3+} will lead to C^{4+}, again emitting an electron. This continues until the ground state is reached. The energy of electrons emitted in a cascade coincides possibly with those of electrons emitted from three- or two-electron capture. Therefore it is expected to find electron target-ion coincidences in the same electron energy range for various target charge states.

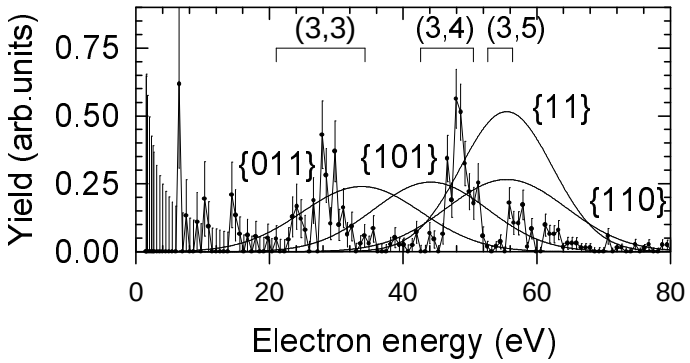

Figure 5.2: Partial electron spectra in coincidence with Ar^{2+}, resulting from collisions of $^{13}C^{6+}$ on Ar. The calculated peak positions and the reaction windows are shown ({11}, indicates that two electrons became quasi-molecular during the collision and both are captured, and {110},{101},{011} indicating that three electrons became quasi-molecular and that *two* have been captured by the projectile).

5.4.1 Ar^{2+}- e^- coincidences

In figure 5.2 the spectrum is plotted of electrons measured in coincidence with Ar^{2+} after collisions of C^{6+}-ions on Ar. The peaks in the measured electron distribution correspond to different initial states of the captured electrons. The electrons measured in this energy range result from decay of the initially populated (3,n) series to the $n = 2$ orbital of C^{5+}. Due to the degeneracy of the two possible final states C^{5+}(2s) and C^{5+}(2p) the energy distributions can be expected to be rather sharp. In table 5.1 the binding energies of several doubly excited states of C^{4+} are summarized. The main contribution of electrons in the spectrum is from electrons initially captured into the (3,4) manifold of C^{4+} which decay subsequently to n=2.

The energies of the (3,4) and (3,5) manifolds coincide with the calculated binding energy for capture of the two outer electrons, i.e. the string {11}. The reaction window corresponding to this string is plotted in figure 5.2. However, in the spectrum we observe not only population of the (3,4) and (3,5) manifold, but also of the (3,3) configurations. The intensity of this structure is much higher than expected from height of the reaction window.

(n_1, n_2)	(3,3)	(3,4)	(3,5)
E_{min}(eV)	88.7	72.5	66.6
E_{max}(eV)	102	80.4	70.3
E^{ai}_{min}(eV)	34.3	50.5	56.4
E^{ai}_{max}(eV)	21.0	42.6	52.7

Table 5.1: Binding energies of the $(3, n)$ manifold of C^{4+} calculated using the Cowan code. Also tabulated in the lower part of the table are the autoionization energies E^{ai} after decay to C^{5+}(2l), which is bound with E_f=123 eV.

In figure 5.2 we have plotted the reaction windows corresponding to the strings {110}, {101}, {011}, i.e. three-electron processes resulting in two-electron capture. The overlap of the string {011} with the observed electrons in the (3,3) manifold indicated that the double electron capture process is accompanied by target excitation.

5.4.2 Ar^{3+} coincidences

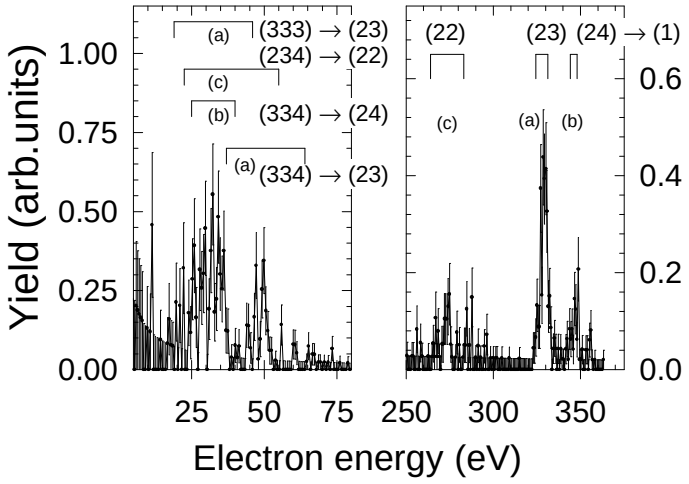

Figure 5.3: In this figure the partial electron spectrum in coincidence with Ar^{3+} is plotted for C^{6+}-Ar collisions. Autoionizing decay of three electrons will be in two steps. For example the decay of (3,3,3) will in the first step of the decay to the (2,3) manifold yield low-energy electrons, the second step is to the n=1 state of the projectile emitting a high energy electron. Peaks indicated with the letter (a), (b) and (c) are ascribed to the corresponding autoionization pathways as plotted in figure 5.4

The partial energy spectrum of electrons in coincidence with Ar^{3+} is plotted in figure 5.3. Autoionizing decay from triply excited states can be separated into two subsequent decay steps.

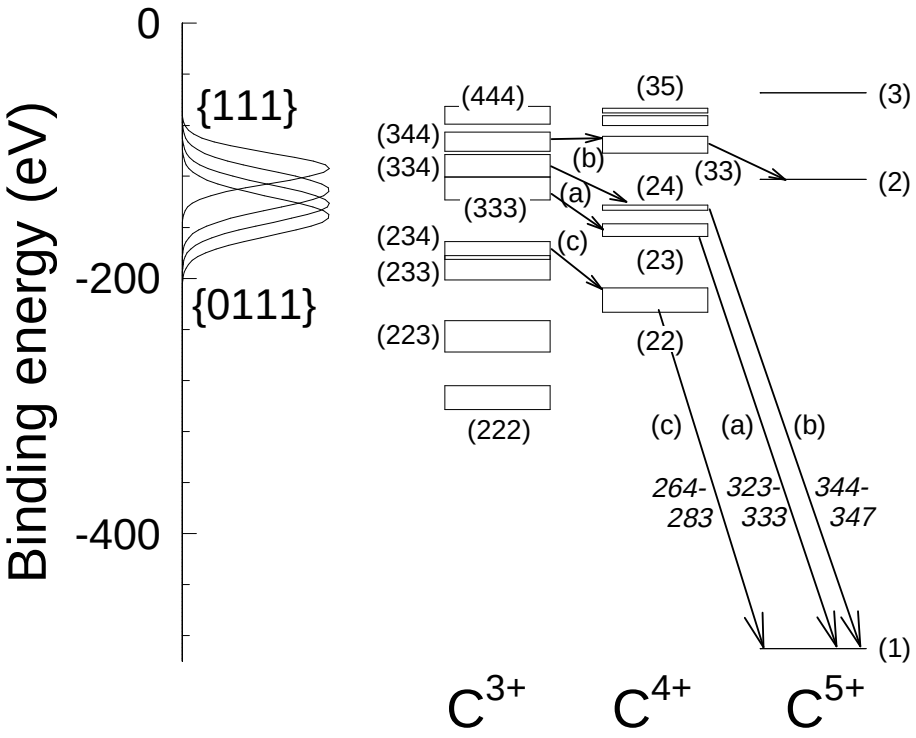

Figure 5.4: Binding energies of different excited states C^{q+}. On the left axis the reaction windows of several strings are plotted for three electron capture. The capture of three electrons will preferably be into (3,3,3) or (3,3,4) configurations. A few autoionizing decay paths are indicated with (a), (b) and (c) yielding the most pronounced peaks in the electron energy spectra in coincidence with Ar^{3+}. In italic the kinetic energy of autoionizing electrons is indicated.

The various decay steps are schematically indicated in figure 5.4. The binding energies of different triply, doubly and singly excited states of C^{3+}, C^{4+} and C^{5+}, respectively, as calculated with the Cowan code, are indicated. The arrows in the figure indicate possible decay steps on basis of the criterion that decay to the nearest continuum is preferred and that two electrons in a manifold interact mutually. The decay pathways indicated with (a), (b) and (c) yield the strongest lines in the spectra of figure 5.3. In figure 5.4 four reaction windows are shown for three-electron capture processes. The reaction window corresponding to the string {111} is centered around 114 eV. This coincides with initial capture into (3,3,4) or (3,3,3) configurations, which decays to the (2,3) manifold, emitting a low energy electron. The second decay step is the decay of (2,3) configurations to (1), the ground state of C^{5+}. In figure 5.3 the range of electron energies for the corresponding autoionization decay in this cascade is indicated with (a).

The observed decay of (2,2)→(1), in the figure indicated with (c), is in our opinion the result of initial capture into the (2,3,4) manifold. This is only possible if also strings like {0111} are involved. The reaction window corresponding to this string is energetically overlapping with the (2,3,4) configurations.

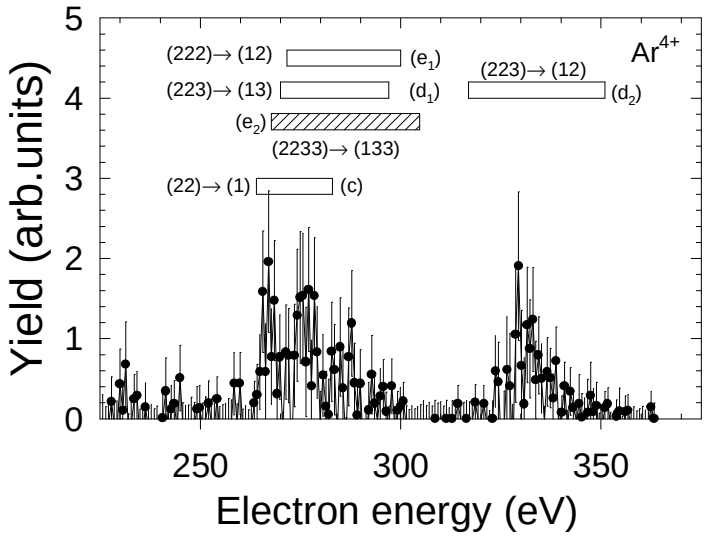

Figure 5.5: Partial electron energy spectrum of electrons in coincidence with Ar^{4+} for high electron energies. In this figure also the autoionizing electron energy of different decay channels is indicated.

5.4.3 Ar^{4+} coincidences

Figure 5.5 shows the spectrum of autoionizing electrons in coincidence with Ar^{4+}. In this spectrum, around 270 eV and 330 eV, two major groups of autoionizing electrons can be identified. Many decay processes yield electrons in this range. To reconstruct from which manifold these electrons originate several

binding energies of multiply excited states in carbon are tabulated in figure 5.6. This figure is an extension of figure 5.4 by adding quadruply excited states of C^{2+}. The figure includes also the relevant reaction windows for four-electron capture, which are positioned at higher binding energies than for the three-electron capture case.

For four-electron capture the overbarrier model predicts for electrons in the string {1111} a total binding energy of 174 eV. The corresponding reaction window is plotted in figure 5.6 and is conform with capture into the (3,3,3,3) or (2,3,3,3) manifolds. Also plotted in this figure are the reaction windows for strings which include target excitation. The transition indicated with (c) can result from initial capture of four electrons in (3,3,3,3) or (2,3,3,3). These configurations will possibly decay to (2,3,3) and subsequently to (2,2) emitting low energy electrons, and as a final step the high energy electron emission from the decay of (2,2)→(1). However, electrons are also observed at quite different energies not covered by this path. Therefore also other transitions must be considered.

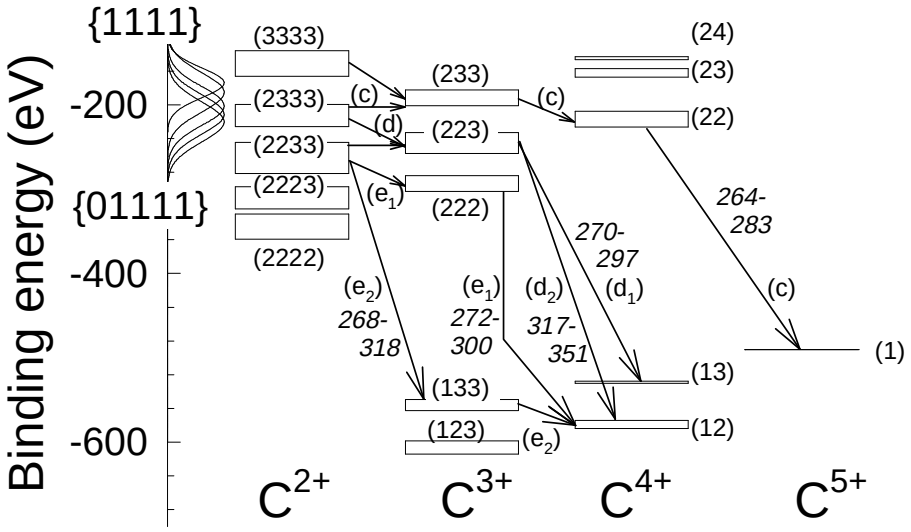

Figure 5.6: Binding energies of various excited states of C^{q+}. On the left axis the reaction windows for several strings are plotted for four electron capture. The capture of four electrons will preferably be into (2,3,3,3) or (3,3,3,3) configurations, which decay autoionizing via paths indicated with (c), (e_i) and (d_i) yielding intensities as seen in the electron energy spectra in coincidence with Ar^{4+}. Indicated in italic is the kinetic energy of an autoionization electron.

The binding energies of the (2,3,3,3) configurations are partially degenerate with (2,3,3). This can be seen by the small overlap in figure 5.6 between these two manifolds. Those of the (2,3,3,3) configurations which are more strongly bound than the (2,3,3) manifold, will decay to (2,2,3), indicated in the figure as (d). The latter can then decay via two different autoionizing steps. Firstly the two electrons in n=2 can interact, yielding (1,3) as a final state (d_1), or in

the second place the electrons in n=2 and n=3 interact which will result in a final state (1,2) (d_2). Transition d_2 yields somewhat higher energy electrons, see figure 5.5 and 5.6.

The assumption of target excitation, described with e.g. the string {01111}, is not in contradiction with the observed electron spectra. For this string, the (2,2,3,3) configurations will probably be populated. This manifold possibly decays via path (e_1) to (2,2,2), which subsequently decays to (1,2) yielding a high energy electron or to (1,3,3) →(1,2), yielding a low energy electron in the second decay step (path e_2). The electron energy range of the latter decay channel is indicated in figure 5.5 as the hatched part.

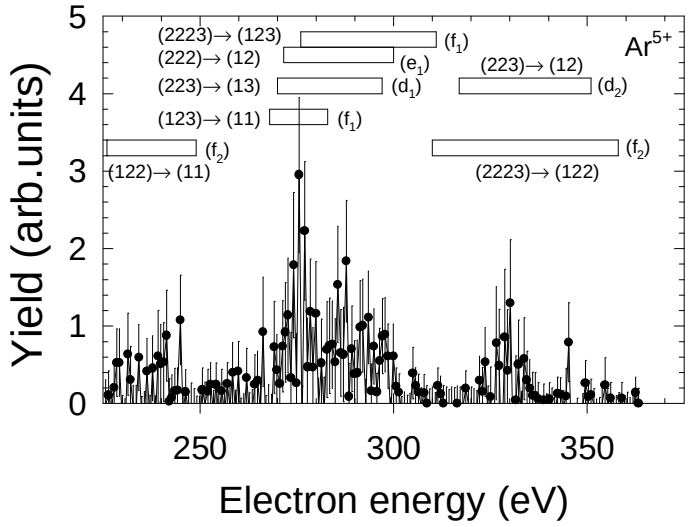

Figure 5.7: Partial electron energy spectrum of electrons in coincidence with Ar^{5+} for high electron energies. In this figure also the autoionizing electron energy of different decay channels is plotted.

5.4.4 Ar^{5+} coincidences

For five-electron capture processes (figure 5.7) it is rather difficult to identify the various electron-capture processes. At first sight the observed autoionizing electrons are in the same energy range as for Ar^{4+} coincidences. Therefore, the observed decay is possibly the same. The difference is that here the observed transition is the second or third step in the decay of C^{1+}. In principle several pathways of autoionizing cascades can contribute to the spectra, partly yielding electrons in the same energy range. The electrons measured in the energy range between 275 and 300 eV can result from the (1,2,3)→(1,1), or the (2,2,2) →(1,2) transition. For each of these two a reconstruction can be made to determine the original level in which the five electrons were captured.

In figure 5.8 the binding energies of some multiply excited states of carbon are presented. Also this figure is an extension of figure 5.6 by adding the five-fold

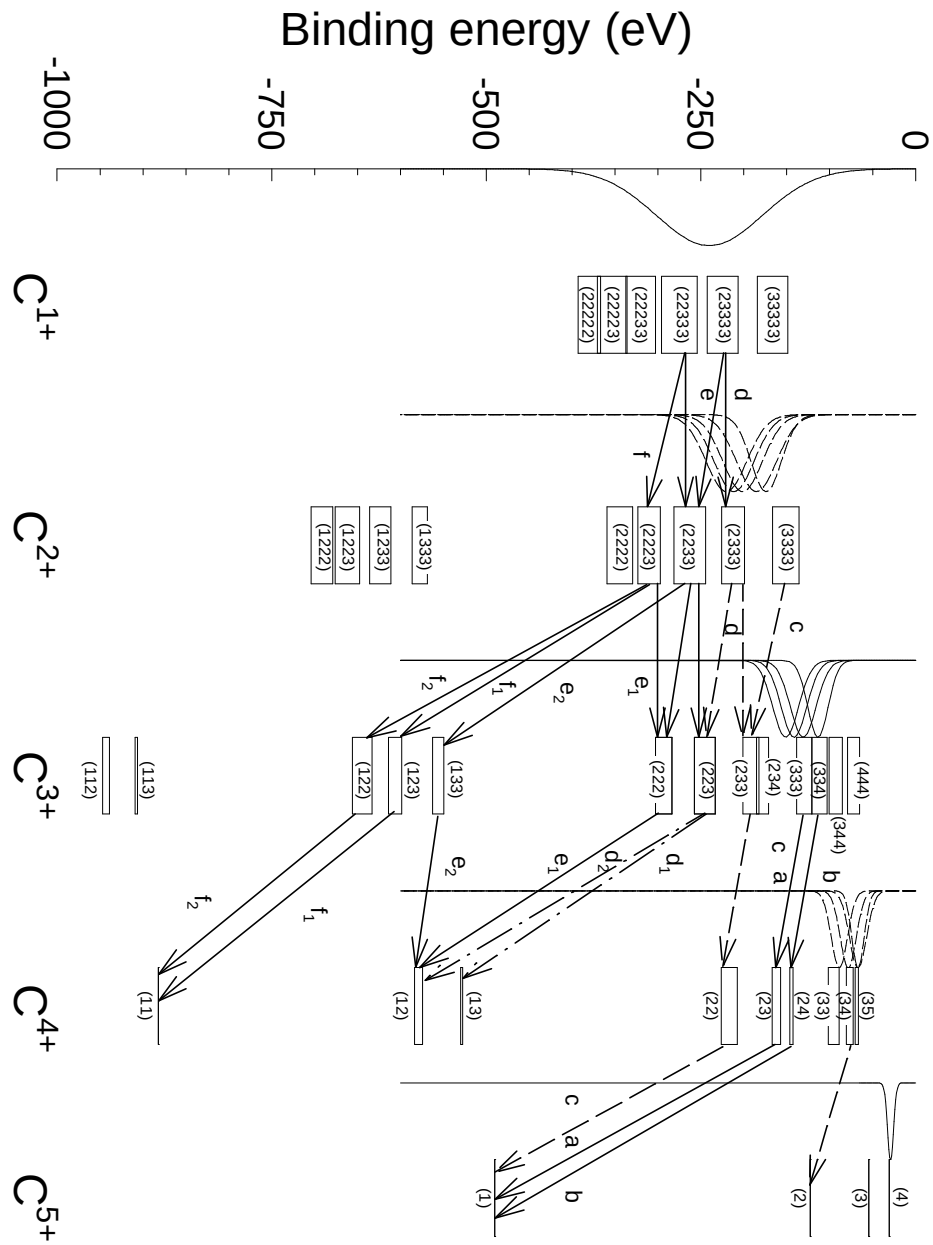

Figure 5.8: The binding energies of various multiply excited states in C^{q+}, q=1..5. The arrows between the boxes indicate autoionizing transitions between the configurations. At the left the reaction windows are plotted for capture of one to five electrons. For clarity the height of all the reaction windows is taken to be equal. Indicated are also the different decay paths.

excited states of carbon. The figure gives an overview of the processes which lead to charge equilibration. For five-electron capture only the cascades starting at the far left part of the figure are relevant. The reaction window plotted for five electron capture corresponds to the {11111} string.

A possible transition between two configurations is indicated with an arrow. Decay (2,2,3)→(1,3), as observed in the electron spectrum (d_1), can originate from initial electron capture in the (2,3,3,3,3) manifold, which then decays to (2,2,3,3) if two of the n=3 electrons interact, and subsequently to (2,2,3). This decay path is indicated with (d). The possible decay of (2,2,3,3)→(2,2,2)→(1,2) in the final step of the decay will yield electrons in the same energy range as (2,2,3)→(1,3).

At the left the reaction window for the string {11111} is plotted. The overlap with the various manifolds is large. Capture of electrons in (2,2,3,3,3) is therefore also possible. The corresponding decay, labeled (e), is indicated in the figure. Autoionization electrons corresponding to this decay can be expected in the range indicated as (e) in figure 5.6.

Different cascades can lead to the same final or intermediate states and this indicates that it is not fully clear into which manifold the electrons are initially captured. Reconstruction allows for a number of initial states of which the binding energies correspond fairly well to the binding energy and range predicted for five electron capture.

5.5 Conclusions

In electron-target ion coincidence measurements for collisions of $^{13}C^{6+}$ on Ar we found that in $^{13}C^{6+}$ - Ar collisions target excitation is an important process. Doubly excited states in collisions between highly charged ions and multi (>2) electron targets are populated via different processes. Besides capture of the two most loosely bound electrons, also capture of two more strongly bound electrons is observed. This latter process results in target excitation and capture in more strongly bound projectile states.

For multi-electron capture it was shown that the observed electrons in the coincidence spectra result from cascading steps after multiple electron capture. The calculations of the overbarrier model are in fair agreement with the binding energies of initially populated states.

Figure 5.8 summarizes the observed electron capture processes and the subsequent pathways. The binding energy of different multiply excited states corresponding to C^{1+} to C^{5+} are plotted, together with the reaction windows for the various capture processes including target excitation. The reaction windows mark the starting manifold for the decay pathways. Indicated with letters are the autoionizing transitions which show up in the electron spectra. Many of the transitions can be traced back almost uniquely to a specific capture process; for example the transitions (1,2,2)→(1,1) and (1,2,3)→(1,1) observed in the decay of C^{3+} (labeled f_1 and f_2) do not originate from three-electron capture but most likely from five-electron capture into C^{1+}(2,2,3,3,3). According to figure 5.8

other transitions such as d_1 and d_2 (2,2,3)→(1,2) or (1,3) can originate from either four- or five-electron capture and indeed transitions d_1 and d_2 are found in the spectra measured in coincidence with Ar^{4+} and Ar^{5+}. So figure 5.8 gives a handle to unfold multiple electron capture in C^{6+}-Ar collisions. Note that one-, two- and three-electron transfer eventually results in C^{5+}-ions, so effectively capturing only one electron, while four- and five- electron transfer leads to two-electron capture, the production of C^{4+}.

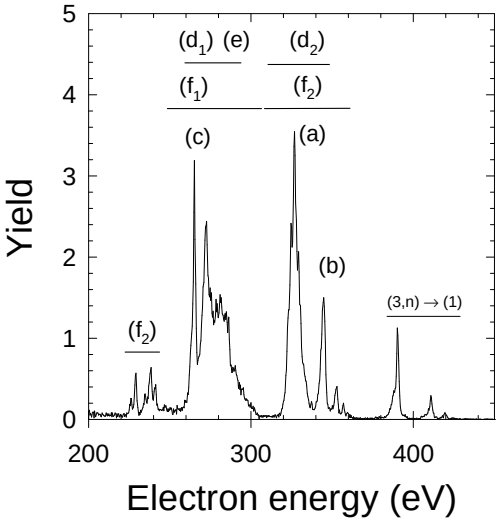

Figure 5.9: In this figure the non-coincident electron energy measurements are plotted (cf 5.1). The letters in the figure represent the energy of different autoionizing cascades steps after multi-electron capture.

In figure 5.9 the high energy part of the non-coincident measurements (figure 5.1) is shown. The letters in the figure indicate, conform figure 5.8, the pathways leading to the emission of high energy electrons. From the coincidence measurements presented in this chapter it is clear that transitions leading to emission of high energy electrons result from capture of different numbers of electrons. For example, the transition (c), which results from three- and four-electron capture, as well as (d_1) corresponding to capture of four or five electrons show up in the same energy range. The figure gives an overview of the peak identifications of the (high energy) autoionization electrons and the corresponding transitions after multi-electron capture.

References

Ali R, Cocke C L, Raphaelian M L A and Stöckli M 1993 *J. Phys. B: At. Mol. Opt. Phys.* **26** L177

Bachau H, Roncin P and Harel C 1992 *J. Phys. B: At. Mol. Opt. Phys.* **25** L109

Bordenave-Montesquieu A, Benoit-Cattin P, Boudjema M, Gleizes A and Bachau H 1987 *J. Phys. B: At. Mol. Opt. Phys.* **20** L695
Chen Z and Lin C D 1993 *Phys. Rev.* A **48** 1298
Cowan R D 1981 *The Theory of Atomic Structure and Spectra* (University of California Press, Berkley, 1981)
Van der Hart H W, Vaeck N and Hansen J 1995 *J. Phys. B: At. Mol. Opt. Phys.* **28** 5207
Van der Hart H W and Hansen J 1994 *J. Phys. B: At. Mol. Opt. Phys.* **27** L395
Mack M, Nijland J H, Van der Straten P, Niehaus A and Morgenstern R 1989 *Phys. Rev.* A **39** 3846
Martin S, Denis A, Delon A, Désesquelles and Ouerdane Y 1993 *Phys. Rev.* A **48** 1171
Niehaus A 1986 *J. Phys. B: At. Mol. Phys.* **19** 2925
De Nijs G, Hoekstra R and Morgenstern R 1994 *J. Phys. B: At. Mol. Opt. Phys.* **27** 2557
De Nijs G, Folkerts H O, Hoekstra R and Morgenstern R 1996 *J. Phys. B: At. Mol. Opt. Phys.* **29** 85
Posthumus J H and Morgenstern R 1992 *Phys. Rev. Lett.* **68** 1315
Posthumus J H, Lukey P and Morgenstern R 1992 *J. Phys. B: At. Mol. Opt. Phys.* **25** 987
Roncin P, Gaboriaud M N and Barat M 1991 *Europhys. Lett.* **16** (6) 551
Roncin P, Gaboriaud M N, Barat M, Bordenave-Montesquieu A, Moretto-Capelle P, Benhenni M, Bachau H and Harel C 1993 *J. Phys. B: At. Mol. Opt. Phys.* **26** 4181